Inorganic Chemistry
Cite This: Inorg. Chem. 2018, 57, 4104−4108
Article
pubs.acs.org/IC

Synthesis of Gadolinium Scandate from a Hydroxide Hydrogel

Ryan J. Paull,[†] Zachary R. Mansley,[†] Tiffany Ly,[†] Laurence D. Marks,[†] and Kenneth R. Poeppelmeier*[,†,‡]

[†]Department of Materials Science & Engineering, Northwestern University, Evanston, Illinois 60208, United States
[‡]Department of Chemistry, Northwestern University, Evanston, Illinois 60208, United States

ABSTRACT: Gadolinium scandate ($GdScO_3$) has been synthesized at 300 °C through the decomposition of a mixed cation hydroxide hydrogel in a humid environment. Increasing the reaction temperature produced larger particles that better adopted the Wulff shape. A lack of water vapor during the synthesis caused the solid network of the hydrogel to collapse upon heating so an amorphous xerogel was produced. Water vapor in the system imbibed the hydrogel and allowed for greater diffusion of the atomic species to allow for crystallization into the perovskite phase at temperatures lower than typical sol−gel processes. Temperatures less than 300 °C, or an excess of water vapor, promoted the formation of $Gd(OH)_3$ and ScOOH in addition to or in lieu of $GdScO_3$.

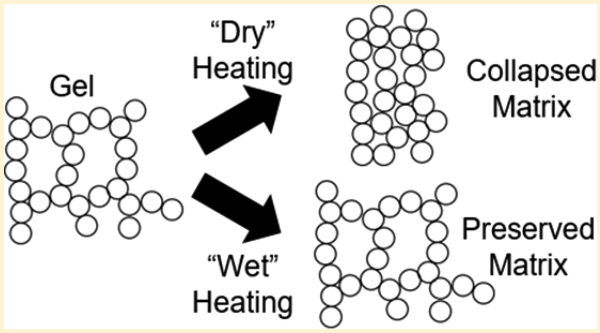

INTRODUCTION

The lanthanide scandates have gained attention for their use as dielectric materials, owing to their high-κ values and large optical band gaps,[1,2] and as substrates for other novel complex oxides since large single crystals can be grown with high purity using different lanthanides to vary the lattice parameter.[2] Bulk lanthanide scandates ($LnScO_3$) form in the orthorhombic perovskite structure with space group *Pbnm* and are alternatively described as pseudocubic with respect to the ⟨110⟩ and ⟨001⟩ directions of the orthorhombic unit cell. This structure features ScO_6 octahedra with an in-phase rotation about the [001] axis and an out-of-phase rotation about the $[1\bar{1}0]$ axis, which is described as $a^-a^-c^+$ in Glazer notation.[3] In particular, $GdScO_3$ has the lattice parameters a = 5.486 Å, b = 5.750 Å, and c = 7.935 Å,[4] which corresponds to a unit cell volume of 250.3 Å^3 containing four formula units and a pseudocubic lattice parameter of 3.970 Å.

These materials have mostly been synthesized as thin films by atomic layer deposition[5] or pulsed laser deposition,[6,7] as single crystals using the Czochralski technique,[2] or as powders through solid-state reactions at high temperatures and/or pressures.[4,8] However, these methods are unsuitable for several applications, such as heterogeneous catalysis, where materials with a high surface area (e.g., oxide nanoparticles) are necessary to attain high catalytic rates in most cases. Producing such materials often requires low reaction temperatures to minimize sintering of particles. Solution-based methods, such as solvothermal synthesis, in which reactions occur in solution in a sealed vessel at temperatures greater than the boiling point of the solution and pressures greater than 1 atm, are common techniques used to obtain materials with high surface area at relatively low temperatures. The solvothermal synthesis of oxides occurs in hydroxide solutions; owing to the negligible solubilities of rare-earth species in alkaline media,[9] there are no reports of synthesizing any $LnScO_3$ through this method.

Another common route is through the creation of an intermediate phase that acts as a precursor that decomposes into a desired phase, but thus far the lowest reported reaction temperature for crystalline $GdScO_3$ using this approach was still relatively high at 850 °C.[10] In this Article we report crystalline $GdScO_3$ synthesized at temperatures as low as 300 °C, the lowest reported temperature for the formation of any crystalline $LnScO_3$, through the decomposition of a mixed cation hydroxide precursor in a humid environment, which we refer to as hydro-sauna conditions. The presence of water vapor enhanced the diffusion of atomic species, allowing for crystallization at lower temperatures than previous sol−gel or precursor-mediated techniques. However, while water is critical for the reaction to proceed, the chemical potential of water must be controlled in order to prevent the formation of additional hydrated or hydroxide phases.

EXPERIMENTAL SECTION

Synthesis. We will describe here the method used to produce $GdScO_3$, returning later to explain why these conditions were used. An equimolar solution of gadolinium and scandium was prepared by dissolving 2 mmol of their sesquioxides in 10 mL of 15.8 N nitric acid maintained at 80 °C and diluting the solution with 10 mL of distilled water. This solution was then added dropwise into 25 mL of 10 M NaOH in an ice bath to precipitate a white mixed cation hydroxide hydrogel, which was then isolated using centrifugation and washed several times with distilled water. This hydrogel, which will be referred to as $GdSc(OH)_6{\cdot}xH_2O$ for convenience, was then used as a precursor for $GdScO_3$ growth. Roughly 700 mg of the hydrogel was sealed in a

Received: January 31, 2018
Published: March 21, 2018

ACS Publications © 2018 American Chemical Society

DOI: 10.1021/acs.inorgchem.8b00281
Inorg. Chem. 2018, 57, 4104−4108

300 mL stainless steel autoclave (Parr 4760) and heated to a reaction temperature between 250 and 450 °C for 2 days. The product was rinsed with distilled water and centrifuged several times, and then it was put into an oven at 80 °C to dry overnight.

Characterization. Simultaneous thermogravimetric and differential thermal analyses (TG-DTA) measurements were performed on a Netzsch Jupiter F3 Simultaneous Thermal Analysis system from room temperature to 550 °C and back at a rate of 10 °C min^{-1} under an air flow of 50 mL min^{-1}. Powder X-ray diffraction (PXRD) was performed on a Rigaku Ultima diffractometer using a Cu K_α source operated at 40 kV and 20 mA. PXRD for Rietveld refinement was performed on a Rigaku Smartlab using a Cu K_α source operated at 45 kV and 160 mA with a 0.02° step size and 1 s dwell time. Raman spectroscopy data was obtained using an inverted microscope (Nikon Eclipse Ti−U) Raman setup as follows: a 632.8 He−Ne laser (Research Electro-Optics, Excelsior 30557) was passed through a short-pass filter to a Nikon Plan Fluor 10×/0.30 objective to the sample on a glass coverslip, and Raman scattering from the sample was back-collected through the microscope objective. Rayleigh scattering was filtered out using a RazorEdge Long Pass U-Grade 633 nm. The filtered light was then focused onto a 1/3 m imaging spectrograph (SP2300, Princeton Instruments), dispersed (1200 grooves/mm grating, 500 nm blaze, centered at 666 nm), and focused onto a liquid nitrogen cooled CCD detector (Spec10:400BR, Princeton Instruments). The power at the sample was 3.38 mW, and the collection time was 108 s. Secondary electron imaging was performed on a Hitachi HD-2300 scanning transmission electron microscope operated at 200 kV.

RESULTS AND DISCUSSION

The formation of crystalline materials requires diffusion so that the atoms may arrange themselves into a lower free-energy periodic structure. In the case of a solid-state reaction, this often requires high temperatures for atoms from one precursor to be able to diffuse into and react with atoms in another precursor. One way around this is through the creation of a precursor in which the ions are already intermixed; through this the atoms are, on average, next to their appropriate neighbor, but a temperature greater than 700 °C is often still required for sufficient diffusion of atoms to produce a crystalline phase.[11] This precursor is often a gel, an amorphous solid network with an encapsulated liquid phase.[12] When a gel is heated, the encapsulated liquid evaporates and the amorphous solid network collapses due to capillary forces (Figure 1),[12] becoming a xerogel, which traps the atoms and prevents

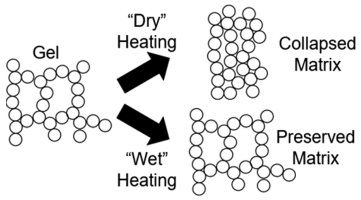

Figure 1. Schematic of a gel before and after heating in both a dry and wet environment. The gel is an amorphous solid network with an encapsulated liquid phase. When heated in a dry environment, the encapsulated liquid phase leaves, and capillary forces cause the solid matrix of the gel to collapse. When heated in a wet environment, the water vapor imbibes the gel to prevent the collapse of the matrix.

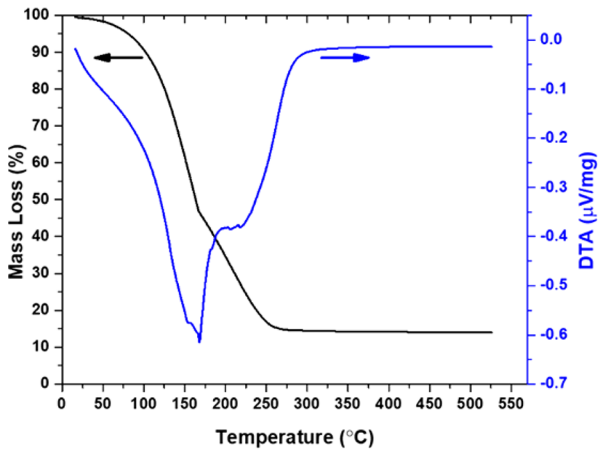

Figure 2. Simultaneous TGA (black) and DTA (blue) curves of the decomposition and dehydration of the $GdSc(OH)_6{\cdot}xH_2O$ hydrogel.

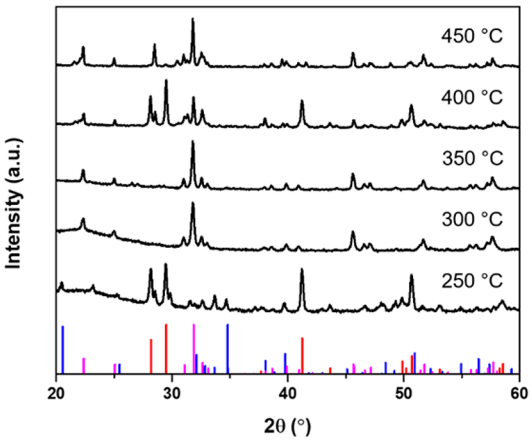

Figure 3. PXRD patterns of the products obtained after heating the gel in an autoclave at (from top to bottom) 450 °C, 400 °C, 350 °C, 300 °C, and 250 °C. The calculated peak locations and relative peak intensity for $GdScO_3$ (pink, PDF 01-074-4353), $Gd(OH)_3$ (red, PDF 01-083-2037), and α-ScOOH (blue, PDF 01-073-1790) are plotted at the bottom. $GdScO_3$ was formed at 300 °C, 350 °C, 400 °C, and 450 °C; $Gd(OH)_3$ and α-ScOOH were formed at 250 °C, 400 °C, and 450 °C.

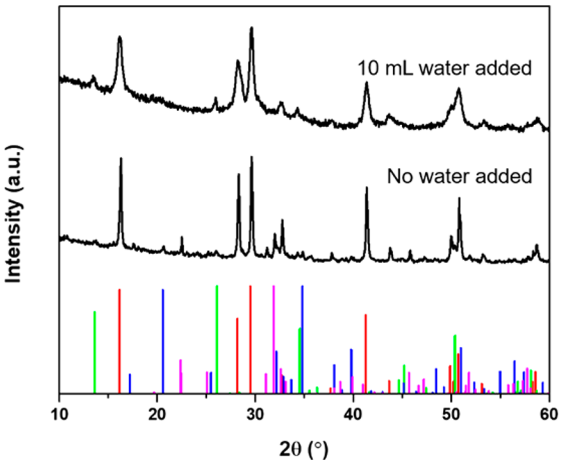

Figure 4. PXRD pattern of the product obtained after heating the gel in an autoclave at 350 °C with (top) 10 mL of distilled water added to the autoclave or (bottom) no additional water. The calculated peak locations and relative peak intensity for $GdScO_3$ (pink, PDF 01-074-4353), $Gd(OH)_3$ (red, PDF 01-083-2037), α-ScOOH (blue, PDF 01-073-1790), and γ-ScOOH (green, PDF 01-072-0360) are plotted at the bottom. The increased amount of gel increased the amount of water and formed more $Gd(OH)_3$ and ScOOH phases as a result, and the addition of water furthered this such that no $GdScO_3$ was formed.

DOI: 10.1021/acs.inorgchem.8b00281
Inorg. Chem. 2018, 57, 4104−4108

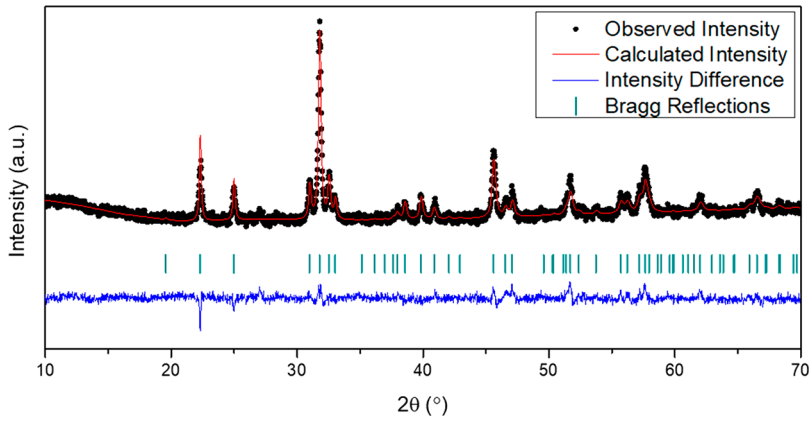

Figure 5. Rietveld refinement plot of the PXRD data for $GdScO_3$ grown in hydro-sauna conditions at 300 °C. Black dots indicate observed data, the red line indicates the calculated pattern, the blue line is the difference between the observed and calculated intensities, and the dark green bars indicate the allowed Bragg reflections for $GdScO_3$.

Table 1. Rietveld Refined Cell Parameters for $GdScO_3$ Produced in Hydro-Sauna Conditions at 300 °C Compared to That of $GdScO_3$ Produced via High-Temperature Solid-State Reactions

Synthesis Method	Hydro-Sauna at 300 °C	High Temperature Solid-State Reaction (PDF 01-074-4353)[4]
a (Å)	5.4864(8)	5.4862(1)
b (Å)	5.7505(9)	5.7499(1)
c (Å)	7.934(13)	7.9345(1)
V (Å^3)	250.33(9)	250.299(5)
Gd^{3+}: *x*	0.013(2)	0.0163(2)
y	0.9403(1)	0.9406(2)
z	0.25000	0.25000
Sc^{3+}: *x*	0	0
y	0.50000	0.50000
z	0	0
O^{2-} (1): *x*	0.888(7)	0.8817(17)
y	0.535(7)	0.5535(18)
z	0.25000	0.25000
O^{2-} (2): *x*	0.699(7)	0.6931(13)
y	0.290(7)	0.3007(14)
z	0.953(5)	0.9444(10)
No. of free parameters	27	46−67
Goodness-of-fit	1.31	1.39
R_p, R_{wp}, R_{exp}	2.8, 3.64, 2.74	3.81, 12.11, 8.72

crystallization except at high temperatures. If the open gel matrix is instead preserved upon heating, sufficient diffusion for crystallization is possible at lower temperatures.

For $GdScO_3$, crystallization was accomplished by decomposing a mixed cation hydroxide hydrogel under hydro-sauna conditions. Rare-earth species have negligible solubilities in basic solutions and readily precipitate out as hydroxides.[9] When the mixed solution of Gd^{3+} and Sc^{3+} was added to a 10 M NaOH solution, a mixed cation hydroxide hydrogel immediately precipitated out. The solid network of the hydroxide hydrogel likely is a random structure containing $Gd(OH)_3$ and $Sc(OH)_3$ units, similar to what is observed in the more well-studied aluminum trihydroxide gel system.[13] The $GdSc(OH)_6 \cdot xH_2O$ hydrogel was characterized using TG-DTA, the results of which are presented in Figure 2. Upon heating to 550 °C, an endothermic reaction occurred and an overall mass loss of 86% was observed. Most of this mass loss may be attributed to

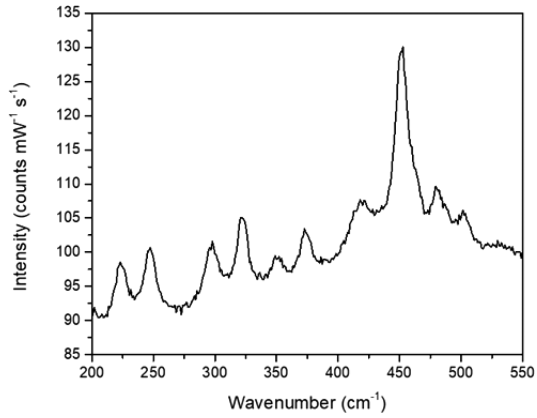

Figure 6. Raman spectrum of $GdScO_3$ grown at 300 °C under hydro-sauna conditions. The 11 peaks are produced due to A_g modes at 248, 321, 418, 452, and 501 cm^{-1}, B_{1g} modes at 223, 373, and 490 cm^{-1}, B_{2g} modes at 298, 351, 463, and 532 cm^{-1}, and B_{3g} modes at 300, 450, and 481 cm^{-1}.

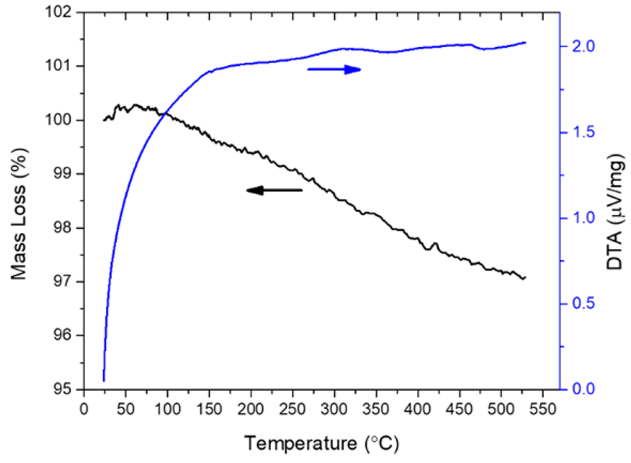

Figure 7. Simultaneous TGA (black) and DTA (blue) curves of $GdScO_3$ grown at 300 °C under hydro-sauna conditions. The constant change in heat and small mass loss suggest the release of water adsorbed on the surface and that hydroxide groups in the material are minimal.

evaporation of water that was encapsulated in the hydrogel, as the dehydration of $GdSc(OH)_6$ alone would only correspond

DOI: 10.1021/acs.inorgchem.8b00281
Inorg. Chem. 2018, 57, 4104−4108

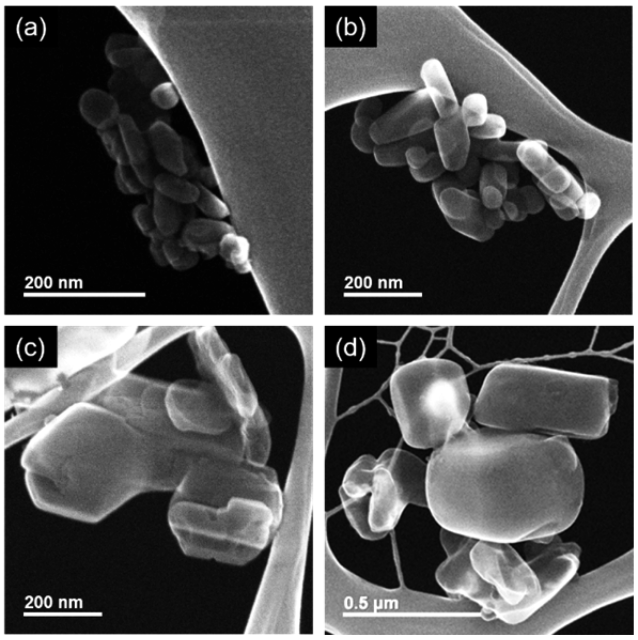

Figure 8. Secondary electron images for the products obtained after heating the gel in an autoclave at (a) 300 °C, (b) 350 °C, (c) 400 °C, and (d) 450 °C.

to a mass loss of 17%. Heating the hydrogel in air to 400 °C fully evaporated the encapsulated water to form a xerogel, trapped the cations, and yielded an amorphous product.

To prevent the collapse of the gel matrix, the hydrogel was heated inside a sealed autoclave; doing so produced water vapor from the evaporation of solvent from the hydrogel, and the presence of this water vapor kept the hydrogel precursor partially imbibed, which allowed for sufficient diffusion for crystallization. PXRD patterns of the products are shown in Figure 3. At 250 °C, the cations segregated into separate phases, namely $Gd(OH)_3$ (PDF 01-083-2037) and α-ScOOH (PDF 01-073-1790), for reasons that will be expanded upon below. At temperatures greater than 300 °C, the PXRD patterns matched predominately with $GdScO_3$ (PDF 01-074-4353). Under these conditions, the precursor can decompose along at least two different reaction pathways depending on the temperature of the reaction:

$$GdSc(OH)_6{\cdot}xH_2O \rightarrow Gd(OH)_3 + ScOOH + (x+1)H_2O \quad (1)$$

$$GdSc(OH)_6{\cdot}xH_2O \rightarrow GdScO_3 + (x+3)H_2O \quad (2)$$

Reducing the free energy of water by raising the temperature (water entropy) or reducing the amount of water will push both reactions 1 and 2 to the right, reaction 2 more so than reaction 1. To explore this in more detail, the effect of the activity of water in the system was investigated. First, ∼10 g of the $GdSc(OH)_6{\cdot}xH_2O$ hydrogel was sealed inside the autoclave and heated to 350 °C for 2 days. The resulting PXRD pattern in Figure 4 shows that this led to less $GdScO_3$ being formed, in favor of $Gd(OH)_3$ and ScOOH, owing to how when a greater amount of gel is sealed inside the autoclave, a greater amount of water is sealed in with it. To further this, an additional 10 mL of distilled water was added to the autoclave again with ∼10 g of the $GdSc(OH)_6{\cdot}xH_2O$ hydrogel and heated to 350 °C for 2 days. The resulting products, as seen by the PXRD pattern in Figure 4, imply that only reaction 1 occurred, as expected. Based on these results, the formation of $Gd(OH)_3$ and α-ScOOH in the products grown at 400 and 450 °C (Figure 3) was attributed to variability in the amount of hydrogel placed in the autoclave; an increase in the amount of hydrogel would increase the amount and activity of water and hence promote reaction 1.

We note that these results explain the failure of simple hydrothermal synthesis of $LnScO_3$; the use of water as a solvent again pushes the reaction toward these hydrated phases. To cross-validate, hydrothermal conditions similar to those previously used for several other rare-earth perovskites, such as $LnCrO_3$,[14] $LnMnO_3$,[15] and $LnFeO_3$,[16] were attempted. To briefly summarize, stoichiometric amounts of $Gd(NO_3)_3{\cdot}6H_2O$ and $ScCl_3{\cdot}6H_2O$ were heated to 250 °C in a high concentration KOH solution ranging from 10 to 20 M. Under these hydrothermal conditions, only $Gd(OH)_3$ and α-ScOOH could be produced, and only $Gd(OH)_3$ formed under sufficiently alkaline conditions (20 M KOH solution) that dissolved the α-ScOOH. Therefore, we conclude that a hydro-sauna treatment in which the water activity can be controlled is necessary to produce perovskite $GdScO_3$.

$GdScO_3$ particles produced via this hydro-sauna synthesis at 300 °C were characterized for their crystalline purity through several techniques. Rietveld refinement of the sample, plotted in Figure 5, showed good agreement with literature values of the lattice parameter and atomic positions of $GdScO_3$ grown by high-temperature solid-state reaction in Table 1. In addition, Raman spectroscopy in Figure 6 was consistent with that of $GdScO_3$ single crystals with the A_g modes at 248, 321, 418, 452, and 501 cm^{-1}, B_{1g} modes at 223, 373, and 490 cm^{-1}, B_{2g} modes at 298, 351, 463, and 532 cm^{-1}, and B_{3g} modes at 300, 450, and 481 cm^{-1}, observed.[17] Simultaneous TG-DTA in Figure 7 showed a constant change in heat and a slow but steady rate of mass loss over a temperature range of 100 to 550 °C and was attributed to the release of water adsorbed on the particle surface. These observations all suggest that $GdScO_3$ of high quality can be synthesized under hydro-sauna conditions at temperatures as low as 300 °C.

The morphology of $GdScO_3$ particles as a function of temperature during hydro-sauna synthesis was characterized using secondary electron imaging in a scanning transmission electron microscope (Figure 8). Reaction temperature had a clear effect on the resulting particle morphology. At 300 °C, particles have no preferential faceting and are small; Scherrer analysis of the PXRD pattern using MDI Jade software determined the average crystallite size to be 63.7 ± 8.7 nm. Since this crystallite size is consistent with the secondary electron image in Figure 8a, peak broadening in the diffraction pattern was assumed to be caused by the crystallite size and not strain. As the temperature increased, the particle size increased past the measurement limit of 100 nm for Scherrer analysis, with particles roughly 100 nm in dimension at 350 °C and up to several hundreds of nanometers by a reaction temperature of 450 °C. In addition, higher temperatures allowed for enough diffusion for the particles to adopt a Wulff shape.[18] Faceting is observed starting at 400 °C. The formation of cuboidal particles at 450 °C implies that the {110} and {001} facets of the orthorhombic perovskite phase, or equivalently the {001} facets of the pseudocubic unit cell, either have the lowest surface energies or have the slowest growth rate normal to them.

DOI: 10.1021/acs.inorgchem.8b00281
Inorg. Chem. 2018, 57, 4104−4108

CONCLUSION

A mixed cation hydroxide gel with water encapsulated within the gel matrix was produced. High surface area particles of $GdScO_3$ were synthesized at low temperatures through the decomposition of this gel in a humid environment. Heating the hydrogel in a dry environment only formed an amorphous product due to the collapse of the open matrix of the gel precursor. An excess of water vapor in the system promoted the formation of (oxy)hydroxide phases, namely $Gd(OH)_3$ and α-ScOOH. $GdScO_3$ was produced with intermediate water vapor pressures at temperatures as low as 300 °C. Higher temperatures increased the diffusion and reaction rates, which favored the formation of larger particles that better adopted a Wulff shape. This method was found to also produce several other $LnScO_3$, $LaScO_3$ and $NdScO_3$ for example, and should be generalizable to other complex oxide materials as well, as an alternative low temperature synthetic route to producing high surface area materials.

AUTHOR INFORMATION

Corresponding Author

*E-mail: krp@northwestern.edu.

ORCID

Ryan J. Paull: 0000-0002-7273-7269

Kenneth R. Poeppelmeier: 0000-0003-1655-9127

Author Contributions

R.J.P. performed the syntheses, powder X-ray diffraction experiments, and simultaneous thermogravimetric and differential thermal analyses. Z.R.M. and T.L. performed secondary electron imaging experiments. R.J.P. performed the majority of the analysis of the experimental results, supervised by L.D.M. and K.R.P. with discussion between all the authors. R.J.P. wrote the first draft of the manuscript, which was refined with input and edits from all authors.

Notes

The authors declare no competing financial interest.

ACKNOWLEDGMENTS

We acknowledge funding from the Northwestern University Institute for Catalysis in Energy Processes (ICEP) on Grant No. DOE DE-FG02-03-ER 15457. ICEP was supported by the Chemical Sciences, Geosciences, and Biosciences Division, Office of Basic Energy Sciences, Office of Science, US Department of Energy.

REFERENCES

(1) Zhao, C.; Witters, T.; Brijs, B.; Bender, H.; Richard, O.; Caymax, M.; Heeg, T.; Schubert, J.; Afanas'ev, V. V.; Stesmans, A.; Schlom, D. G. Ternary rare-earth metal oxide high-k layers on silicon oxide. *Appl. Phys. Lett.* **2005**, *86* (13), 132903.

(2) Uecker, R.; Velickov, B.; Klimm, D.; Bertram, R.; Bernhagen, M.; Rabe, M.; Albrecht, M.; Fornari, R.; Schlom, D. G. Properties of rare-earth scandate single crystals (Re = Nd−Dy). *J. Cryst. Growth* **2008**, *310* (10), 2649−2658.

(3) Glazer, A. The classification of tilted octahedra in perovskites. *Acta Crystallogr., Sect. B: Struct. Crystallogr. Cryst. Chem.* **1972**, *28* (11), 3384−3392.

(4) Liferovich, R. P.; Mitchell, R. H. A structural study of ternary lanthanide orthoscandate perovskites. *J. Solid State Chem.* **2004**, *177* (6), 2188−2197.

(5) Myllymaki, P.; Roeckerath, M.; Lopes, J. M.; Schubert, J.; Mizohata, K.; Putkonen, M.; Niinisto, L. Rare earth scandate thin films by atomic layer deposition: effect of the rare earth cation size. *J. Mater. Chem.* **2010**, *20* (20), 4207−4212.

(6) Christen, H. M.; Jellison, G. E.; Ohkubo, I.; Huang, S.; Reeves, M. E.; Cicerrella, E.; Freeouf, J. L.; Jia, Y.; Schlom, D. G. Dielectric and optical properties of epitaxial rare-earth scandate films and their crystallization behavior. *Appl. Phys. Lett.* **2006**, *88* (26), 262906.

(7) Iacopetti, S.; Shekhter, P.; Winter, R.; Tromm, T. C. U.; Schubert, J.; Eizenberg, M. The asymmetric band structure and electrical behavior of the $GdScO_3$/GaN system. *J. Appl. Phys.* **2017**, *121* (20), 205303.

(8) Amanyan, S. N.; Arsen'ev, P. A.; Bagdasarov, K. S.; Kevorkov, A. M.; Korolev, D. I.; Potemkin, A. V.; Femin, V. V. Synthesis and examination of $GdScO_3$ single crystals activated by Nd^{3+}. *J. Appl. Spectrosc.* **1983**, *38* (3), 343−348.

(9) Moeller, T.; Kremers, H. E. The basicity characteristics of scandium, yttrium, and the rare earth elements. *Chem. Rev.* **1945**, *37* (1), 97−159.

(10) Grover, V.; Shukla, R.; Jain, D.; Deshpande, S. K.; Arya, A.; Pillai, C. G. S.; Tyagi, A. K. Complex $GdSc_{1-x}In_xO_3$ oxides: synthesis and structure driven tunable electrical properties. *Chem. Mater.* **2012**, *24* (11), 2186−2196.

(11) Perthuis, H.; Colomban, P. Sol-gel routes leading to nasicon ceramics. *Ceram. Int.* **1986**, *12* (1), 39−52.

(12) Brinker, C. J.; Scherer, G. W. *Sol-Gel Science: The Physics and Chemistry of Sol-Gel Processing*; Academic Press: San Diego, 1990; p 912.

(13) Nail, S. L.; White, J. L.; Hem, S. L. Structure of aluminum hydroxide gel I: initial precipitate. *J. Pharm. Sci.* **1976**, *65* (8), 1188−1191.

(14) Wang, S.; Huang, K.; Hou, C.; Yuan, L.; Wu, X.; Lu, D. Low temperature hydrothermal synthesis, structure and magnetic properties of $RECrO_3$ (RE = La, Pr, Nd, Sm). *Dalton Trans.* **2015**, *44* (39), 17201−17208.

(15) Wang, Y.; Lu, X.; Chen, Y.; Chi, F.; Feng, S.; Liu, X. Hydrothermal synthesis of two perovskite rare-earth manganites, $HoMnO_3$ and $DyMnO_3$. *J. Solid State Chem.* **2005**, *178* (4), 1317−1320.

(16) Zhou, Z.; Guo, L.; Yang, H.; Liu, Q.; Ye, F. Hydrothermal synthesis and magnetic properties of multiferroic rare-earth orthoferrites. *J. Alloys Compd.* **2014**, *583*, 21−31.

(17) Chaix-Pluchery, O.; Kreisel, J. Raman scattering of perovskite $DyScO_3$ and $GdScO_3$ single crystals. *J. Phys.: Condens. Matter* **2009**, *21* (17), 175901.

(18) Wulff, G. On the question of speed of growth and dissolution of crystal surfaces. *Z. Krystallogr.* **1901**, *34*, 449−530.

DOI: 10.1021/acs.inorgchem.8b00281
Inorg. Chem. 2018, 57, 4104−4108